

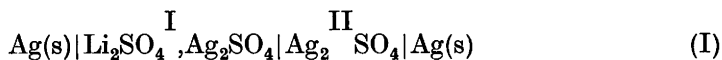
## Determination of the Phase Diagram $\text{Li}_2\text{SO}_4\text{-Ag}_2\text{SO}_4$ from Concentration Cell Measurements

HARALD A. ØYE

*Institutt for uorganisk kjemi, Norges tekniske høgskole, Trondheim, Norway\**

The phase diagram for the system  $\text{Li}_2\text{SO}_4\text{-Ag}_2\text{SO}_4$  is established from investigations of the concentration cell  $\text{Ag} | (\text{Li}_2\text{SO}_4, \text{Ag}_2\text{SO}_4)_{\text{mix}} | \text{Ag}_2\text{SO}_4 | \text{Ag}$ . The concentration cell method has proved very accurate in the determination of phase transitions. No true compound is found between the two components, but three different high-temperature phases, each with a wide homogeneity range, are described.

Various investigations by Førland and Krogh-Moe of the systems  $\text{Na}_2\text{SO}_4\text{-K}_2\text{SO}_4$ <sup>1</sup> and  $\text{Li}_2\text{SO}_4\text{-Na}_2\text{SO}_4$ <sup>2</sup> as well as of pure  $\text{Li}_2\text{SO}_4$ <sup>3</sup> have revealed solid high-temperature modifications that appear to have a high degree of disorder and a high electrical conductance. A detailed knowledge of such highly disordered solids facilitates the understanding of the thermodynamic and structural properties of the molten state. From the phase diagrams of Nacken<sup>4</sup> it was expected that the system  $\text{Li}_2\text{SO}_4\text{-Ag}_2\text{SO}_4$  would have one or more high-temperature solid phases with similar properties, and this system was chosen for a detailed study because of the possibility of establishing reversible Ag electrodes and utilizing the cell:



The system  $\text{Li}_2\text{SO}_4\text{-Ag}_2\text{SO}_4$  was investigated by Nacken<sup>4</sup> more than fifty years ago by means of thermal analysis, but the resulting phase diagram had an odd appearance which in spite of Nacken's careful work called for a reinvestigation. Concentration cells of the type



where A and B are metals and AX a salt, have been used for the determination of phase relationships in metallic systems, for instance by Strickler *et al.*<sup>5</sup> and a number of other authors. It appears from the literature that the reverse

\* Temporary address: Chemistry Division, Argonne National Laboratory, Argonne, Illinois, U.S.A.

method, using a concentration cell with two identical electrodes to investigate the phase diagram of the electrolyte system, has scarcely been used. It also seemed that the system  $\text{Li}_2\text{SO}_4\text{--Ag}_2\text{SO}_4$  should be well suited for this method. Thus, the accurate establishment of the phase diagram for this system by means of EMF measurements became the first object of this investigation.

Apart from the inherent interest in the specific system studied, it was felt that the investigation would also contribute to the general establishment of the potentialities and limitations of the concentration cell method for obtaining thermodynamic information on ionic mixtures.

### PRINCIPLES

The concentration cell I was decided utilized for the evaluation of the phase diagram of the system  $\text{Li}_2\text{SO}_4\text{--Ag}_2\text{SO}_4$ .

The EMF of a cell with transference has been derived by several authors. A form especially convenient for cell I is given by Førland.<sup>6</sup>

$$\Delta E = -\frac{1}{2F} \int_{\text{I}}^{\text{II}} \frac{t'_{\text{Li}^+}}{N_{\text{Li}^+}} d\mu_{\text{Ag}_2\text{SO}_4} \quad (\text{const } T) \quad (1a)$$

or defining

$$\Delta\psi = -F\Delta E = \frac{1}{2} \int_{\text{I}}^{\text{II}} \frac{t'_{\text{Li}^+}}{N_{\text{Li}^+}} d\mu_{\text{Ag}_2\text{SO}_4} \quad (\text{const } T) \quad (1b)$$

$F$  is the Faraday constant.  $t'_{\text{Li}^+}$  denotes the electrochemical transport number of  $\text{Li}^+$  relative to the  $\text{SO}_4^{2-}$  ions and  $N_{\text{Li}^+}$  is the ion fraction of  $\text{Li}^+$ .  $\mu$  is used for the partial free enthalpy. In the mixture  $\text{Li}_2\text{SO}_4\text{--Ag}_2\text{SO}_4$  which has a common anion we will for convenience use the notation

$$\mu_{\text{Ag}^+} = \frac{1}{2}\mu_{\text{Ag}_2\text{SO}_4}$$

and for the following general discussions we use  $\text{A}^+$  and  $\text{B}^+$  for  $\text{Ag}^+$  and  $\text{Li}^+$ , respectively.

$$\Delta\psi = \int_{\text{I}}^{\text{II}} \frac{t'_{\text{B}^+}}{N_{\text{B}^+}} d\mu_{\text{A}^+} \quad (\text{const } T) \quad (2)$$

The phase diagram for the condensed system  $\text{AY--BY}$  can be determined from  $\Delta\mu(T, N_{\text{A}^+})$ . The determination of phase diagrams by concentration cell measurements is in principle a static method, *i.e.*, the temperature is kept constant and  $\Delta\psi$  is measured when equilibrium is attained. The phase diagram is then obtained from plots of  $\Delta\psi$  as a function of temperature and composition.

It is also possible, however, to determine phase transitions by a dynamic method. From concentration cell measurements at constant heating or cooling rate, all phase changes in the mixtures causing heat effects, will appear as humps on the curve  $\Delta\psi(T)_{N_{\text{A}^+}}$ , due to the formation of thermocells.

In the following we assume that  $\Delta\psi(T, N_{\text{A}^+})$  is known, and the influence of phase transitions on  $\Delta\psi(N_{\text{A}^+})_T$  and  $\Delta\psi(T)_{N_{\text{A}^+}}$  will be demonstrated.

*Identification of two-phase regions in the phase diagram.* For a condensed binary system,  $(\Delta\mu_{A+})_T$  is independent of concentration within a two-phase region. From eqn. (1b) it can be seen that  $\Delta\psi(N_{A+})_T$  will remain constant in the two-phase region as well.

It is not implied that the transport numbers are equal in the two phases which are in equilibrium. If they differ, one of the phases is formed at the cost of the other by the transport process. But as  $\Delta\psi_{A+}$  is equal for the two phases the reaction represents no chemical work.

In a one-phase region,  $\Delta\psi(N_{A+})_T$  varies with the composition and the phase boundary lines are obtained from a plot of  $\Delta\psi(N_{A+})_T$  against  $N_{A+}$ , or better  $\ln N_{A+}$  (see for example Fig. 11).

*Determination of boundaries between a one-phase region and a two-phase region.* The function  $\Delta\psi(T)_{N_{A+}}$  in general will not be a constant in a two-phase region, but a plot of the function *versus*  $T$  will exhibit a break when passing from a one-phase to a two-phase region. This may be denoted by writing  $\Delta\psi = \Delta\psi'$  in the one-phase region and  $\Delta\psi = \Delta\psi''$  in the two-phase region.  $\Delta\psi$  is continuous so that  $\Delta\psi' = \Delta\psi''$  at the boundary between the two regions.

The relationship  $\Delta\psi'(\ln N_{A+})_T$  is assumed linear in the vicinity of the phase boundary line,

$$\Delta\psi'(N_{A+})_T = a \ln N_{A+} + C \quad (3a)$$

$$\left(\frac{\partial \Delta\psi'}{\partial N_{A+}}\right) = \frac{a}{N_{A+}} \quad (3b)$$

where  $a$  and  $C$  are constants.

Along the phase boundary line (Fig. 1)

$$\begin{aligned} d\Delta\psi &= \left(\frac{\partial \Delta\psi'}{\partial T}\right)_{N_{A+}} dT + \left(\frac{\partial \Delta\psi'}{\partial N_{A+}}\right)_T dN_{A+} \\ &= \left(\frac{\partial \Delta\psi''}{\partial N_{A+}}\right)_T dN_{A+} + \left(\frac{\partial \Delta\psi''}{\partial T}\right)_{N_{A+}} dT \end{aligned} \quad (4a)$$

Furthermore  $\left(\frac{\partial \Delta\psi''}{\partial N_{A+}}\right)_T = 0$  because of equilibrium.

Using eqn. (3b)

$$\left(\frac{\partial \Delta\psi'}{\partial T}\right)_{N_{A+}} dT + \frac{a}{N_{A+}} dN_{A+} = \left(\frac{\partial \Delta\psi''}{\partial T}\right)_{N_{A+}} dT \quad (4b)$$

$$\frac{dN_{A+}}{dT} = \left[ \left(\frac{\partial \Delta\psi''}{\partial T}\right)_{N_{A+}} - \left(\frac{\partial \Delta\psi'}{\partial T}\right)_{N_{A+}} \right] \frac{N_{A+}}{a} \quad (4c)$$

$dN_{A+}/dT$  is the slope of the phase boundary line in the phase diagram of the condensed binary system. Eqn. (4c) shows that when a phase boundary between a one-phase and a two-phase region is passed,  $\Delta\psi(T)_{N_{A+}}$  will always show a break since  $dN_{A+}/dT \neq 0$ . The equation can be used to calculate the slope of the phase boundary line, when the magnitude of the break in  $\Delta\psi(T)_{N_{A+}}$  is known.

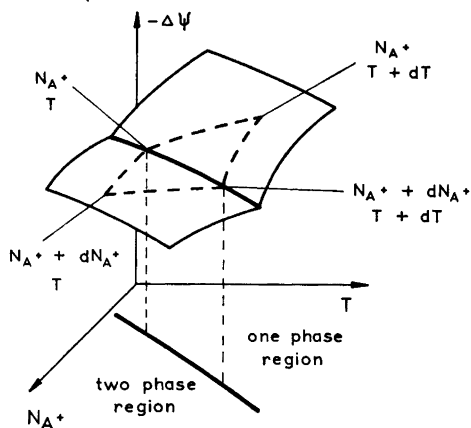


Fig. 1. Illustration of the relationship between  $N_{A^+}$ ,  $T$  and  $\Delta\psi$  along a boundary line between a one-phase and a two-phase region. The projection in the  $(N_{A^+}-T)$  plane represents the phase boundary line in a condensed binary phase diagram.

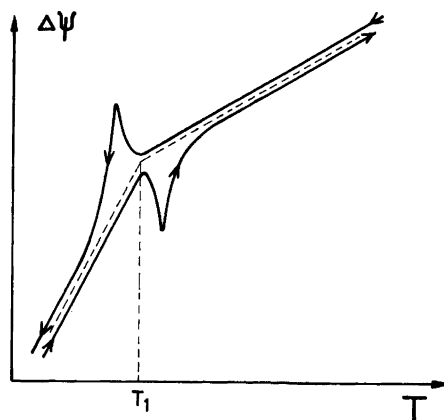


Fig. 2.  $\Delta\psi(T)_{N_{A^+}}$ . The passage of the boundary between two two-phase regions when the temperature is uniformly varied.

*Determination of the boundary between two two-phase regions.* In a binary phase diagram with  $T$  as the ordinate and the composition as the abscissa, the boundary between two two-phase regions will always be horizontal or vertical.  $\Delta\psi(T)_{N_{A^+}}$  generally shows a break on passing a horizontal phase boundary.

If the cell  $A|(AY, BY)_{\text{mix}}|AY|A$  is heated at a constant rate, an additional effect will be observed when the boundary line between two two-phase regions is passed. A two-phase/two-phase transition will take place. One of the two phases disappears and simultaneously a new one is being formed. This reaction is endothermic and a halt in the temperature will occur in the left half cell. A thermocell is established, and consequently a hump on the experimentally determined  $\Delta\psi(T)_{N_{A^+}}$  curve is observed. The opposite effect will be observed if the system is cooled (Fig. 2). The size of the humps depends on the heats of reaction and the rate of heating or cooling of the cell.

This thermocell effect is quite analogous to the effect which is observed by differential thermal analysis. A two-phase/two-phase transition is easily observed because this represents an integral reaction on the phase line. A one-phase/two-phase transition, on the other hand, is in principle a differential reaction and this transition will be observed in thermal analysis only if the rate of temperature variation is quite large.

## EXPERIMENTAL

The concentration cell investigation was performed in two steps. At first, solid mixtures of  $\text{Li}_2\text{SO}_4$  and  $\text{Ag}_2\text{SO}_4$  were investigated over the whole concentration range. Then the solid-liquid transformations and liquid mixtures were studied. Three different types of cells were used, depending on temperature and concentration range.

*Experimental set-up.* The experimental set-up is shown in Fig. 3. The furnace resembles the "general purpose laboratory furnace" used in this laboratory. Details of its construction have been given by Motzfeldt.<sup>7</sup>

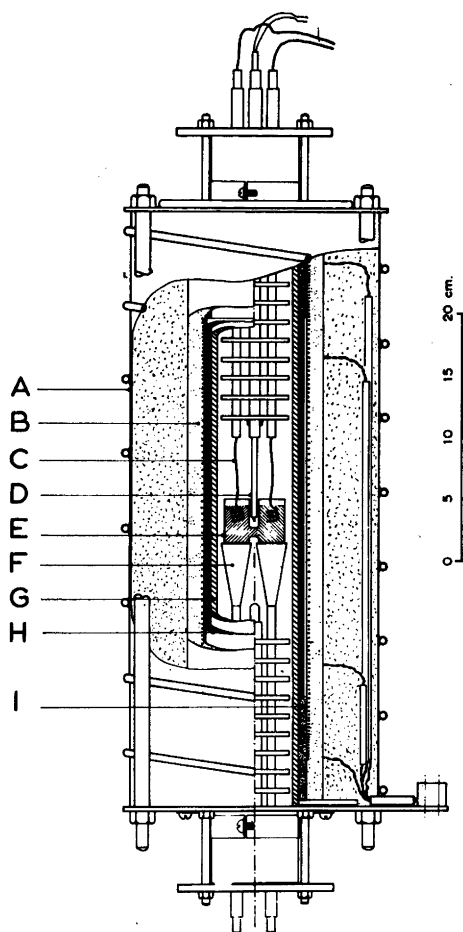


*Fig. 3.* Diagram of furnace and equipment. A. Water cooled furnace jacket. B. Kanthal heating element. C. Ag-electrodes. D. Pt/Pt10Rh thermocouple. E. Quartz glass cell. F. Cell supporter. G. Pythagoras furnace tube. H. Copper tube. I. Petrol coke.

The H-shaped cell (E) was placed on supporters (F) made of refractory tubes and alumina cement. The cells normally used had internal resistance between 10 and 1000  $\Omega$  above the temperatures where the high-temperature modifications were formed. The low-temperature modifications of  $\text{Li}_2\text{SO}_4$  and  $\text{Ag}_2\text{SO}_4$  have low conductivities like most ionic solids. The solid high-temperature mixtures, however, have conductivities more like fused salts and almost no abrupt increase in the conductivities is observed when the solid mixtures melt.

All experiments were performed in air, as the use of an inert or protective gas was found unnecessary.

The measurements were performed within the temperature range 400–900°C. At the lower temperatures the heat exchange by radiation is small, and hence it is difficult to obtain a zone of uniform temperature in the middle of the furnace. A thick-walled copper tube (H) placed outside the furnace tube was used to overcome this trouble. The heating

element (B), made of Kanthal A wire (A. B. Kanthal, Hallstahammar, Sweden) embedded in alumina cement, was placed outside the copper tube. To prevent oxidation of the copper tube (H), the dead space between the Pythagoras tube (F) and the Kanthal element (B) was filled with petrol coke.

The heating element was built in three sections.<sup>7</sup> By regulating the power separately to each section, it was possible to obtain uniform temperature within  $\pm 0.5^\circ\text{C}$  along the middle 12 cm of the furnace chamber.

Constant temperature was obtained by using a voltage stabilizer (Type 100-2 S, Sorensen Ardag, Zürich, Switzerland) for the power supply to the furnace.

The temperature was measured with a Pt/Pt10Rh thermocouple (D), the hot junction placed close to the cell and at the same level. In the investigation of the solid mixtures, the hot junction was left unprotected to insure a minimum time lag. When fused mixtures were employed, the junction was enclosed in an  $\text{Al}_2\text{O}_3$  protection tube.

Ice and distilled water in a vacuum bottle were used for the cold junction. The temperature was determined to an accuracy of  $\pm 0.1^\circ\text{C}$  by means of a precision potentiometer (Thermo-Electric Free Potentiometer, Diesselhorst Pattern, Type 3589 R. H. Tinsley and Co., Ltd., London, England) and a mirror galvanometer with resistance  $15\ \Omega$  (Multiflex-Galvanometer Type MG O, Dr. B. Lange, Berlin, Germany).

The thermocouple wires were annealed according to the direction given by the National Bureau of Standards,<sup>8</sup> and calibrated against the melting points of aluminum and silver. All temperature readings were corrected according to this calibration.

The silver electrodes were welded to copper wires outside the furnace. To prevent possible thermovoltage, the silver/copper junctions were placed in a separate vacuum bottle. The cell potential was determined by means of a potentiometer (Type A-212-A Elektrometer, Trondheim, Norway) with a Multiflex mirror galvanometer, the potentiometer being calibrated against the Tinsley precision potentiometer. The readings were usually performed to an accuracy better than one part in ten thousand.

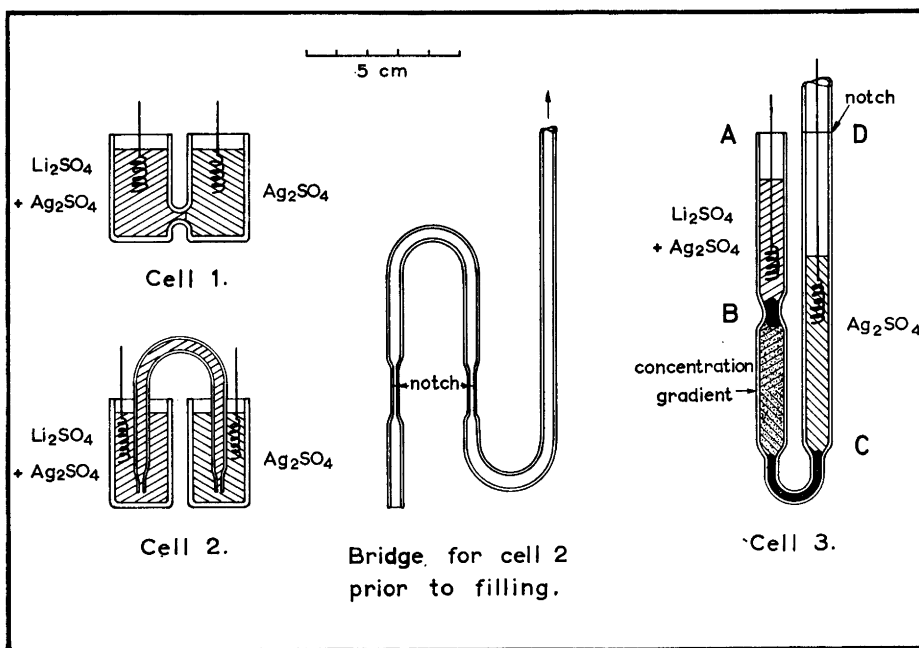


Fig. 4. Quartz cells used for the concentration cell measurements.

**Chemicals.** The electrodes were 0.8 mm silver wire, purity 99.998 % (Johnson and Matthey Ltd., London, England). The  $\text{Li}_2\text{SO}_4$  used was Analar quality, formula  $\text{Li}_2\text{SO}_4 \cdot \text{H}_2\text{O}$  (Hopkin and Williams, Chadwell Heath, England). The crystals were dried for at least 2 h at about  $140^\circ\text{C}$  and were then considered free from water.  $\text{Ag}_2\text{SO}_4$  Analar quality (Hopkin and Williams) was used for the investigations of solid mixtures of  $\text{Li}_2\text{SO}_4$  and  $\text{Ag}_2\text{SO}_4$ . Later on a special quality  $\text{Ag}_2\text{SO}_4$  cryst. (Merck, Darmstadt, Germany) was used. The total amount of impurities were less than 0.2 % (water not included) for both qualities. The Merck quality contained 0.5 % water. After drying at  $180^\circ\text{C}$  about 0.2 % water remained. The last 0.2 % were removed, however, when the  $\text{Ag}_2\text{SO}_4$  was melted. The weighings were corrected for the water. The  $\text{Ag}_2\text{SO}_4$  (Hopkin and Williams) was yellowish when melted, while the  $\text{Ag}_2\text{SO}_4$  (Merck) turned a little more brown. The darkening of the  $\text{Ag}_2\text{SO}_4$  was probably due to a slight decomposition as the remaining water was driven off. By a simple experiment, the solubility of Ag in  $\text{Ag}_2\text{SO}_4$  was determined to be not more than 0.2 wt % (and possibly much less).

In a concentration cell experiment, mixtures prepared from the two qualities of  $\text{Ag}_2\text{SO}_4$  to the same composition were tested against each other. No detectable potential difference was found, and both chemicals were therefore considered to be of satisfactory purity.

**Charging the cells.**  $\text{Li}_2\text{SO}_4$  showed no sign of decomposition within the investigated temperature range (up to  $900^\circ\text{C}$ ).  $\text{Ag}_2\text{SO}_4$ , however, is much more unstable. Hegedüs and Fukker<sup>9</sup> report a starting decomposition in air at  $790^\circ\text{C}$ , in good agreement with the observations made by the author.\*

\* The thermal decomposition of  $\text{Ag}_2\text{SO}_4$  probably goes to Ag,  $\text{O}_2$  and  $\text{SO}_3$ , with a very low solubility of the oxide in the melt. Hence the "temperature of starting decomposition" *i.e.*, the temperature at which the total gas pressure reaches 1 atm, would be a more definite quantity in this case than, *e.g.*, in the case of alkali sulphates or carbonates.

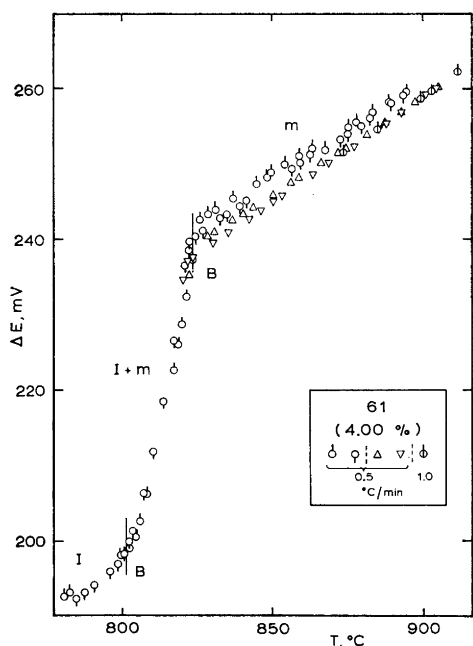


Fig. 5.

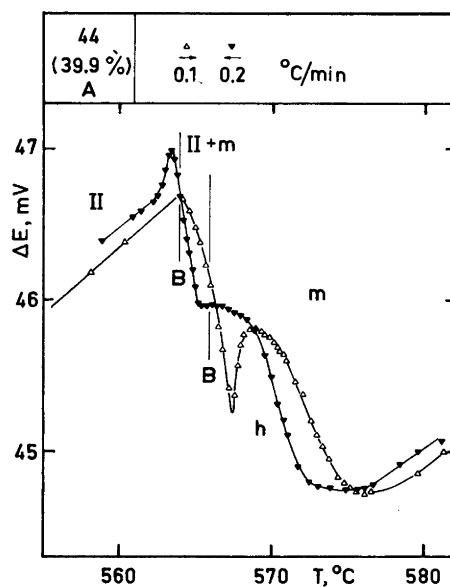


Fig. 6.

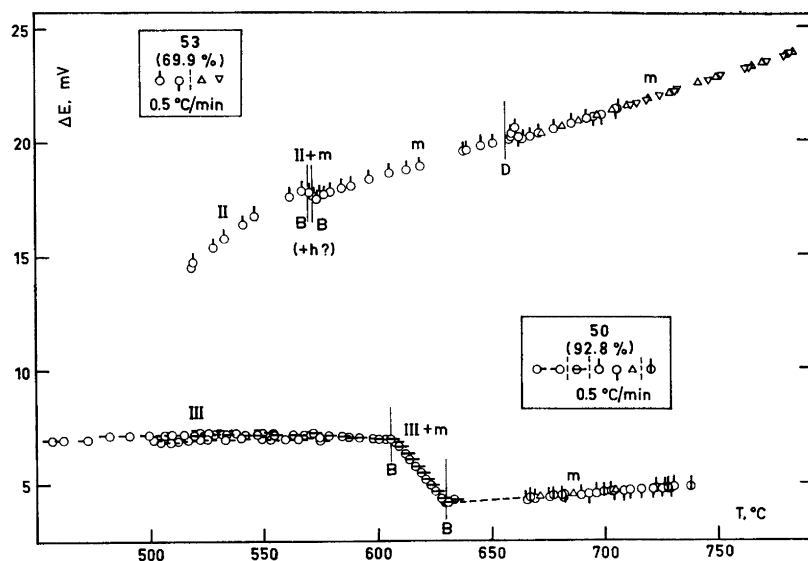


Fig. 7.

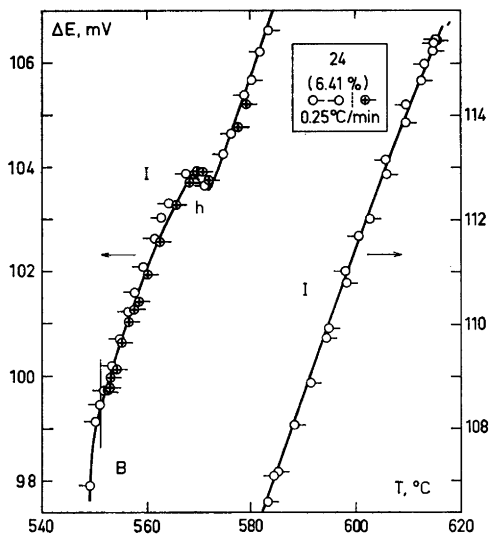


Fig. 8.

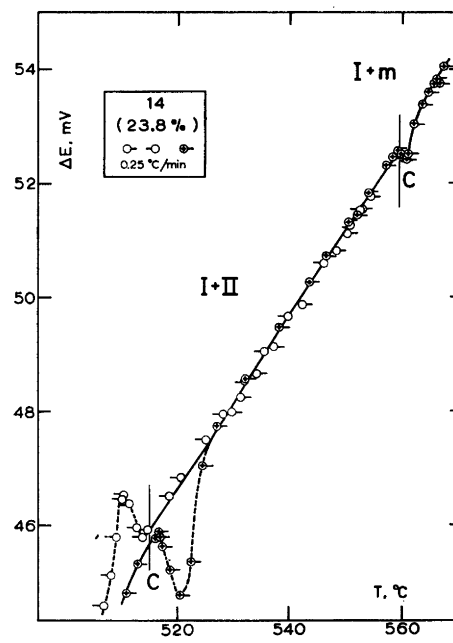


Fig. 9.



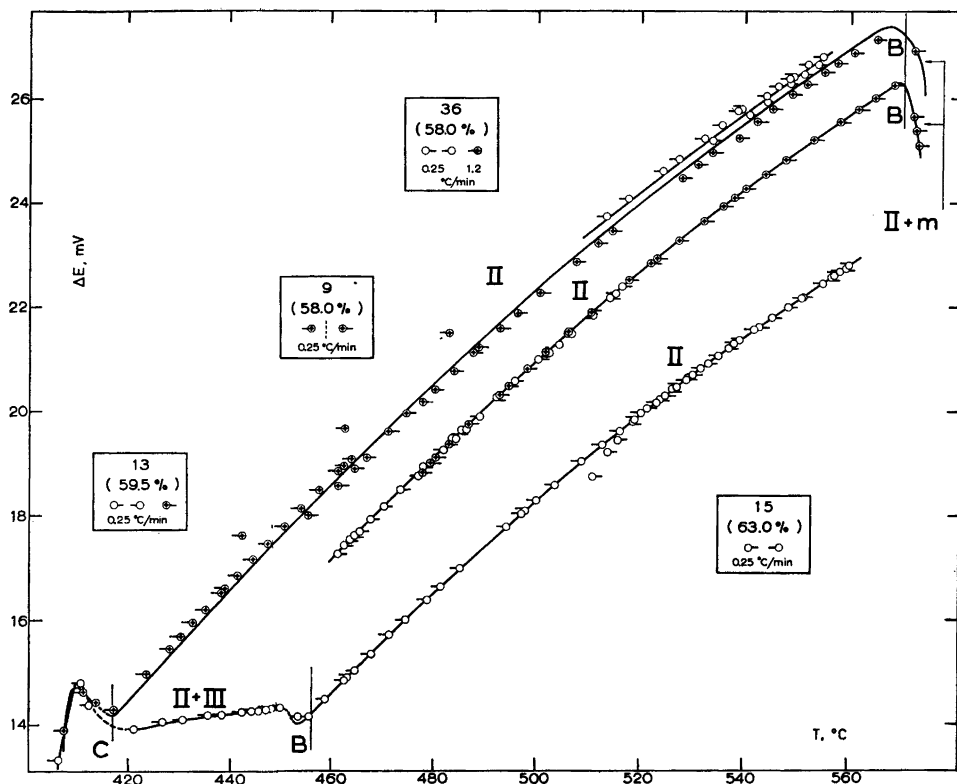


Fig. 10.

Figs. 5—10. Measured potential  $\Delta E$  for the cell



1. Symbols used in the frame.

No. of experiment.

Composition of mixture in mole %  $\text{Ag}_2\text{SO}_4$ .

The different symbols used are given in order of appearance. Values measured at a constant rate of heating: Marks pointing upward or to the right. Values measured at a constant rate of cooling: Marks pointing downwards or to the left.

∴ The cell left overnight. (Could result in some diffusion).

The rate of temperature variation is given in  $^{\circ}\text{C}/\text{min}$ .

2. Symbols used below the curve.

A. One-phase/two-phase transition (Fig. 11).

B. One-phase/two-phase transition giving a simple break.

C. Two-phase/two-phase transition. Break, accompanied by a hump due to thermo-cell formation. The hump point upwards by cooling and downwards by heating.

D. Melting of the standard state, pure  $\text{Ag}_2\text{SO}_4$ . Break, accompanied by a thermo-cell hump being opposite to what is observed for C.

h. Hump observed in the temperature range  $559\text{--}576^{\circ}\text{C}$  for all cells when the composition of the mixture is less than 80 mole %  $\text{Ag}_2\text{SO}_4$  (cf. Figs. 6 and 8). This hump is not considered due to a phase transition in the mixture in the left half-cell. It will be explained later.

3. Symbols used above the curve.

Above the curve phases present are given. The symbols refer to the resulting phase diagram in Fig. 12.

The  $\text{Li}_2\text{SO}_4$ – $\text{Ag}_2\text{SO}_4$  mixture and the pure  $\text{Ag}_2\text{SO}_4$  were filled into the cell in the molten state. A quartz crucible filled with a molten mixture of  $\text{Li}_2\text{SO}_4$  and  $\text{Ag}_2\text{SO}_4$  will crack if cooled to the temperature range where the  $\beta$ -modifications of the salts are formed.

To avoid decomposition, the filling process for the mixtures was as follows:

Mixtures with 25–100 mole %  $\text{Ag}_2\text{SO}_4$  were made by first mixing the two components well at room temperature in a quartz crucible. The mixture was then heated to around 700°C where melting occurred. After some additional stirring, the mixture was filled into the cell.

Mixtures in the range 1–25 mole % were prepared by first melting pure  $\text{Ag}_2\text{SO}_4$  at 700°C. The melt was allowed to cool down to room temperature and then broken in lumps. Pure  $\text{Li}_2\text{SO}_4$  was melted at 900°C and a lump of  $\text{Ag}_2\text{SO}_4$  dropped into the melt. The  $\text{Ag}_2\text{SO}_4$  melted and dissolved quickly. After some stirring the cell was filled. By this procedure  $\text{Ag}_2\text{SO}_4$  was not kept above 700°C for any length of time. In the dilute mixture the  $\text{Ag}_2\text{SO}_4$  is more stable. (A rough calculation based on estimated data, shows that in a mixture with 1 mole %  $\text{Ag}_2\text{SO}_4$ , the dissociation pressure of  $\text{Ag}_2\text{SO}_4$  is lowered corresponding to a temperature decrease of 100°C).

All cells were made of quartz glass. Three different types were used (Fig. 4). Cell 1 was used for the investigation of solid mixtures. A silver electrode was placed in the left half-cell and molten  $\text{Li}_2\text{SO}_4$ – $\text{Ag}_2\text{SO}_4$  then poured into it. An iron rod was put into the right half-cell against the communicating tube, preventing the melt from running into this part of the cell. After the mixture had solidified, the cell was placed into the furnace, which had a temperature between 400°C and 550°C, and left overnight in order to smooth out concentration gradients.

The right half-cell was then fitted with a silver electrode and filled with pure molten  $\text{Ag}_2\text{SO}_4$ , the cell assembly returned to the furnace, and after 20 min the measurements were started. The electrodes were wound into spirals, thus giving a larger surface in order to diminish the effect of concentration gradients, and were kept at some distance from the communicating tube between the two half-cells to diminish the influence of diffusion on the measurements. This simple arrangement functioned well, the potential change being less than 1 % in 24 h at constant temperature.

Cell 2 was used for the investigation of mixtures between 1 and 20 mole %  $\text{Ag}_2\text{SO}_4$  in the temperature range 500–640°C. In the concentration gradient, mixtures between 35 and 80 mole %  $\text{Ag}_2\text{SO}_4$  melt above 576°C. The bridge prevented this melting from spreading, thus preventing a complete mixing and melting of the two electrolytes.

The fused  $\text{Li}_2\text{SO}_4$ – $\text{Ag}_2\text{SO}_4$  mixture was sucked into the bridge (Fig. 4). After solidification of the melt, the bridge was broken at the notches. The bridge and an electrode were placed in the left cell and the cell was then filled up with the mixture used in the bridge. When the melt had solidified, the cell was placed into the furnace and kept there overnight to smooth out possible concentration gradients. The next day the other side of the bridge was put into another cell which was filled with pure  $\text{Ag}_2\text{SO}_4$ . The cell was left for 20 min in the furnace before the measurements started.

Neither of the cells mentioned above could be used for molten electrolytes. For investigations of solid-liquid transformations and liquid mixtures, cells of type 3 were used. From B to C the cell was filled with pure  $\text{SiO}_2$  (–72 + 150 mesh), stoppered at the ends with quartz-wool. The  $\text{Li}_2\text{SO}_4$ – $\text{Ag}_2\text{SO}_4$  mixture was filled into the tube AB. The cell was placed in a separate pot-furnace where the mixture was kept liquid. The elongated end was connected to a vacuum pump and the mixture was sucked down to C. The cell was then removed from the pot-furnace and broken at the notch. Pure  $\text{Ag}_2\text{SO}_4$  was filled into CD. For solid salts at 25°C, the densities of  $\text{Li}_2\text{SO}_4$  and  $\text{Ag}_2\text{SO}_4$  are: 2.22 g/cm<sup>3</sup> and 5.45 g/cm<sup>3</sup>, respectively. The amount was adjusted so that the static liquid pressure of the pure  $\text{Ag}_2\text{SO}_4$  in CD was a little higher than the corresponding pressure of the mixture in CA. When liquidostatic equilibrium then was attained, the concentration gradient was in the middle of BC, thus minimizing diffusion.

The supporter with the cell was then placed into the furnace as shown in Fig. 3. The measurements were started after 10–20 min.

*Determination of the cell potential.* The EMF of the cell reached the equilibrium value very rapidly, *i.e.*, as soon as equality of temperature within the cell was established. It was therefore decided to perform the corresponding EMF and temperature readings at a constant rate of temperature change.

$\Delta\psi$  for a certain temperature was measured both at a constant rate of heating and at a constant rate of cooling; the former value was normally found to be slightly lower than the latter. This was due to a delay of temperature fall or rise between the cell and the hot junction of the thermocouple. By first measuring  $\Delta\psi$  at constant heating and then later at constant cooling rate, the equilibrium values of  $\Delta\psi(T)_{N_{\text{Ag}}^+}$  were obtained by interpolation. In most experiments, however, the differences were quite small (see for instance Fig. 10).

The determination of  $\Delta\psi$  and  $\partial\Delta\psi/\partial T$  at a constant rate of temperature change had the advantages that a time dependent diffusion could easily be corrected for. In the solid solution the diffusion was negligible and the curves for heating and cooling were parallel. In the cells with liquid mixtures, however, a small time dependent diffusion had to be corrected for.

$\partial\Delta\psi/\partial T$  was then taken as the mean value between the cooling and the heating value. (The diffusion effect is illustrated on Fig. 5).

The investigations of the solid solutions were generally carried out at a heating/cooling rate of 0.25°C/min, the liquid mixtures at 0.5°C/min. Heating/cooling rates as low as 0.05°C/min were used in the study of some details.

*Determination of the transition point depression of  $\text{Ag}_2\text{SO}_4$ .* The transition point depression of  $\text{Ag}_2\text{SO}_4$  was determined by heating cells of type 1. The values obtained by cooling were considered inaccurate due to considerable supercooling of  $\alpha\text{-Ag}_2\text{SO}_4$ .<sup>10</sup>

The resistance of this cell was about  $10^6 \Omega$ , hence a galvanometer with high internal resistance was used (Multiflex, resistance  $2 \times 10^4 \Omega$ ).

*Determination of the liquidus line by thermal analysis (cooling curves).* Between 35 and 80 mole %  $\text{Ag}_2\text{SO}_4$  the liquidus line determined from the concentration cell measurements disagrees with the results obtained by Lesnykh *et al.*<sup>11</sup>, determined by differential thermal analysis. To confirm the present results, the liquidus line was redetermined by thermal analysis.

The same "general purpose laboratory furnace" was used (Fig. 3), except for a slight change in supporter design. An  $\text{Al}_2\text{O}_3$  crucible of volume 100 ml was used. First a mixture of 36.0 mole %  $\text{Ag}_2\text{SO}_4$ , total amount 86 g, was prepared. Mixtures of higher  $\text{Ag}_2\text{SO}_4$  contents were made by successively adding more  $\text{Ag}_2\text{SO}_4$  to the previous mixture. The melt was continuously stirred by means of an  $\text{Al}_2\text{O}_3$  tube, cut to a helix at the lower end. Temperature measurements were performed by a Pt/Pt10Rh thermocouple protected by a closed  $\text{Al}_2\text{O}_3$  tube. The cooling rate was 0.2–0.3°C/min. The supercooling was not more than 0.1°C.

## EXPERIMENTAL DATA

Figs. 5–10 are a representative selection of experimental curves for  $\Delta E(T)_{N_{\text{Ag}}^+} = -\frac{1}{F} \Delta\psi(T)_{N_{\text{Ag}}^+}$  and may serve for illustration of the construction of the phase diagram. The investigation is far more comprehensive than necessary for the determination of the phase diagram, since the purpose was also to determine the thermodynamic functions of the mixtures.

To get an accurate determination of a phase transition it was necessary to have close readings in the neighbourhood of the transition. To make the figures more legible, however, some of these readings are omitted.

For cells with mixtures from 1–80 mole % the potential shows a complex variation with temperature around 570°C. This phenomenon was separately investigated and an example is shown in enlarged scale in Fig. 6.

Fig. 11 is constructed from a series of experiments and shows the variations of the potential with composition.

On Fig. 12 the phase diagram is constructed by correlating the experimental observations by the three principles discussed in PRINCIPLES.

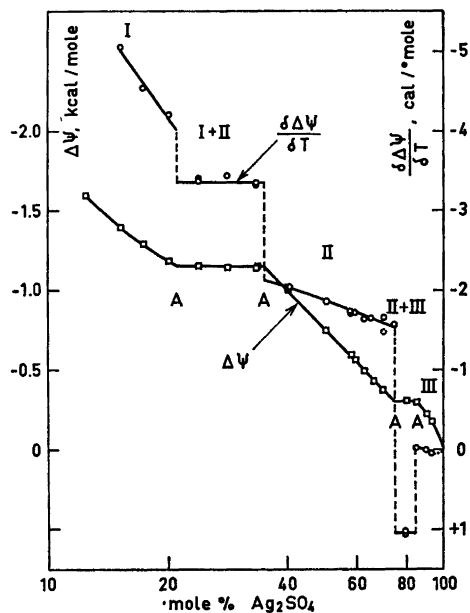


Fig. 11.  $\Delta\psi$  and  $\partial\Delta\psi/\partial T$  for solid mixtures of  $\text{Li}_2\text{SO}_4$  and  $\text{Ag}_2\text{SO}_4$  at  $540^\circ\text{C}$ .

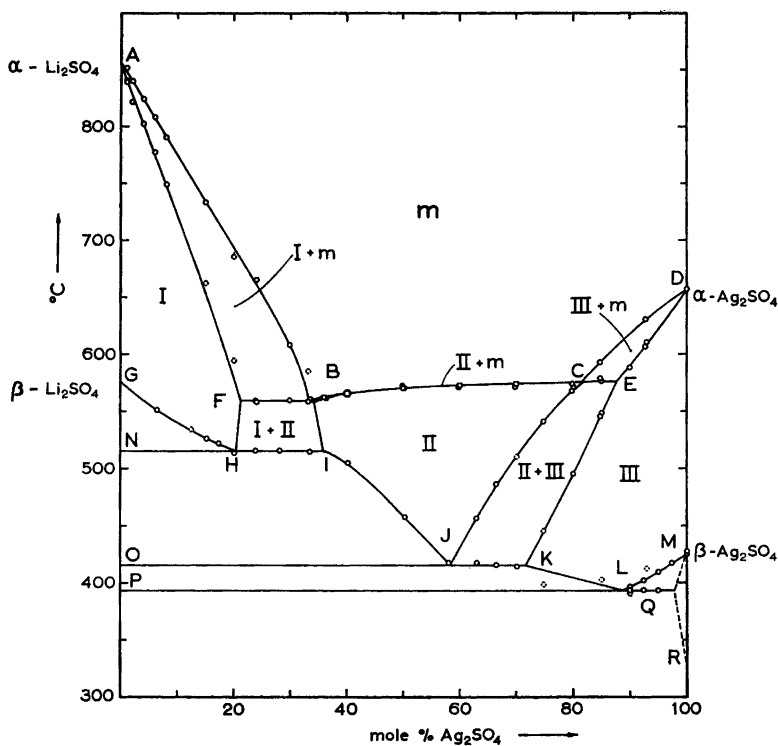


Fig. 12. The phase diagram  $\text{Li}_2\text{SO}_4$ - $\text{Ag}_2\text{SO}_4$  from this investigation.  $\circ$  Concentration cell measurements.  $\square$  Thermal analysis of cooling curves.

With heating and cooling rates of 0.25 to 0.5°C/min the values obtained by heating usually were 2°C higher than those obtained by cooling. When only one set of values was determined, 1°C was subtracted or added respectively. When both values were measured, the mean value was used.

The limits of error, estimated from the reproducibility and uncertainty in the interpolation to the transition temperature, was usually in the range  $\pm 1$  to  $\pm 2^\circ\text{C}$ . The liquidus line for  $0.36 < N_{\text{Ag}^+} < 0.80$  was also determined by thermal analysis with a precision of  $\pm 0.3^\circ\text{C}$ .

Three types of solid solutions at high temperatures are observed, denoted I, II, and III.

A limited solid solubility of  $\text{Li}_2\text{SO}_4$  in  $\beta\text{-Ag}_2\text{SO}_4$  possibly exists. When 90.0 and 95.0 mole %  $\text{Ag}_2\text{SO}_4$  were measured against pure  $\text{Ag}_2\text{SO}_4$ , the cell potential still was 2 mV at the eutectic temperature 393°C, but the EMF of the cell  $\text{Ag}|92.4 \text{ mole \% } \text{Ag}_2\text{SO}_4|97.4 \text{ mole \% } \text{Ag}_2\text{SO}_4|\text{Ag}$  was approximately zero at the eutectic temperature.

#### CALCULATIONS

The nearly vertical boundaries for the phase region (I + II) are difficult to determine by direct measurement of  $\Delta\psi(T)_{N_{\text{Ag}^+}}$ . These boundaries are instead found indirectly from a plot of the function  $\Delta\psi(N_{\text{Ag}^+})_T$  as given in Fig. 11. From the difference in  $(\partial\Delta\psi/\partial T)_{N_{\text{Ag}^+}}$  the slope of the phase line can be calculated from eqn. (4c). The values found for  $T = 540^\circ\text{C}$  are:

Left phase boundary:

$$N_{\text{Ag}^+} = 0.210 \text{ and } dN_{\text{Ag}^+}/dT = 1.8 \times 10^{-4} (\text{C})^{-1}$$

Right phase boundary:

$$N_{\text{Ag}^+} = 0.350 \text{ and } dN_{\text{Ag}^+}/dT = 3.9 \times 10^{-4} (\text{C})^{-1}$$

A similar procedure may be used for the boundaries of region (II + III) (*cf.* right-hand part of Fig. 11) in good agreement with the directly determined boundaries.

The solidus and liquidus lines for phase II (concentration range 35 to 80 mole %  $\text{Ag}_2\text{SO}_4$ ) are surprisingly close together. The maximum temperature difference as found by direct measurement of  $\Delta\psi(T)_{N_{\text{Ag}^+}}$  was around 3°C. Because of the nearly horizontal course of these phase boundaries, a more accurate determination may be done by calculating the difference in concentration at constant temperature, utilizing the liquidus line which was determined to within  $\pm 0.3^\circ\text{C}$  by thermal analysis. The difference between the solidus and the liquidus was found to be 1°C for 36 mole %  $\text{Ag}_2\text{SO}_4$  decreasing to 0.05°C for 80 mole %  $\text{Ag}_2\text{SO}_4$ .

The hump denoted h occurring in the temperature range 559–576°C for cells with mixtures from 1 to 80 mole % is not due to a phase change in the mixture, as the following observations indicate:

(a) By assuming a phase change taking place the construction of a thermodynamically consistent phase diagram seemed impossible.

(b) In cells with mixtures between 35 and 80 mole %  $\text{Ag}_2\text{SO}_4$  the hump occurs above the liquidus temperature determined by thermal analysis.

(c) The solid solutions between 1 and 20 mole %  $\text{Ag}_2\text{SO}_4$  were investigated separately by means of high temperature X-ray diffraction<sup>12</sup> and by qualitative

conductivity measurements. When  $d$ -spacings or conductivity were plotted against the temperature  $T$ , no break appeared in the range 559–576°C.

The hump is considered due to a strongly temperature dependent junction potential in this temperature range. As an example the following cell is considered:

Ag|6.41 mole %  $\text{Ag}_2\text{SO}_4$ |100 mole %  $\text{Ag}_2\text{SO}_4$ |Ag. This cell has a potential given by eqn. (2). Because of the special form of the phase diagram, all mixtures in the concentration gradient between 35 and 80 mole % are solid at 559°C while they at 576°C are liquid. When the transport numbers are different in the solid and in the liquid mixtures, a hump will result in this temperature range. A calculation has been carried out which shows that the hump is explained by assuming  $t'_{\text{Li}^+}$  to decrease 5 % from the solid to the liquid mixtures.

#### DISCUSSION OF THE PROPOSED PHASE DIAGRAM FOR THE SYSTEM $\text{Li}_2\text{SO}_4$ – $\text{Ag}_2\text{SO}_4$

The phase diagram constructed from the present investigation was shown in Fig. 12. The same diagram, but with the present experimental points omitted, has been reproduced in Fig. 13 where the experimental points of Nacken<sup>4</sup>

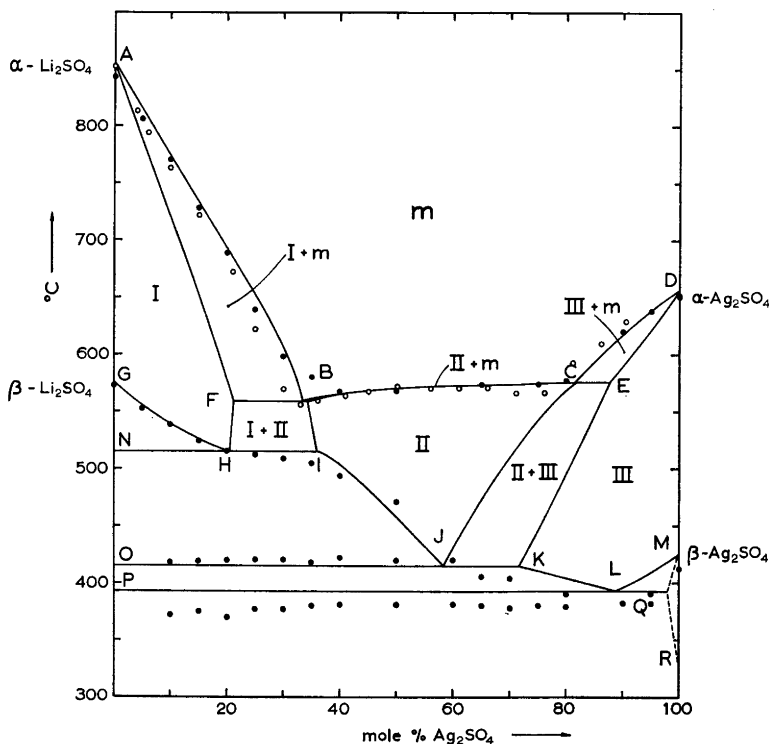


Fig. 13. The phase diagram constructed from this investigation (heavy lines) compared with previous experimental results. ● Nacken<sup>4</sup>. ○ Lesnykh *et al.*<sup>11</sup>

and of Lesnykh *et al.*<sup>11</sup> have been plotted for comparison. The agreement in experimental observations is seen to be fairly satisfactory, whereas the conclusions drawn are rather different.

Lesnykh assumed eutectics at 31.5 and 75 mole %  $\text{Ag}_2\text{SO}_4$  and a congruent melting compound  $\text{Li}_2\text{SO}_4 \cdot \text{Ag}_2\text{SO}_4$ . The results obtained by the present author by thermal analysis and concentration cell measurements give no indication of the compound.

The present investigation agrees well with the observations of Nacken, whose phase diagram is reproduced in Fig. 14. The thermal analysis method

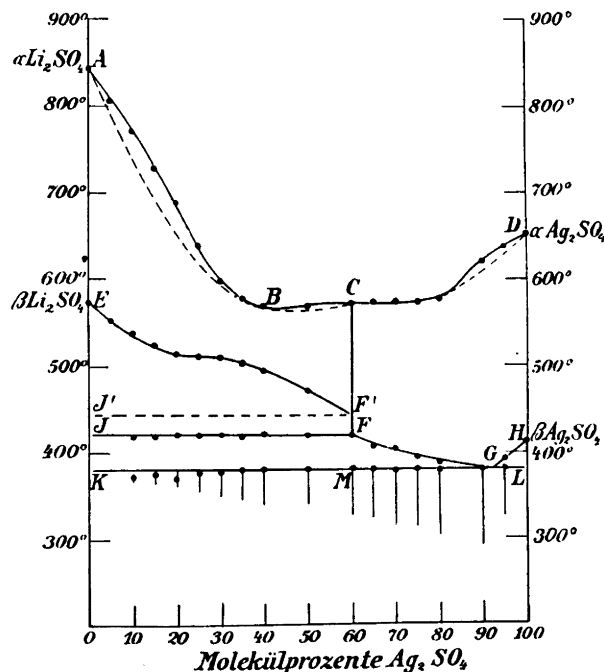


Fig. 14. Phase diagram constructed by Nacken<sup>4</sup> from his experimental results.

applied by Nacken was, however, not sensitive enough to detect all the transitions taking place in the solid solutions. He was thus unable to record the transition from phase I to phase II and the transition from phase II to phase III.

Nacken assumed that only two different solid solutions and a compound  $2\text{Li}_2\text{SO}_4 \cdot 3\text{Ag}_2\text{SO}_4$  existed. In his thorough discussion he admits that the shape of the liquidus line was not sufficient proof for the existence of the compound. Nevertheless, he supported his belief in the existence of the compound by the fact that the line  $\text{EF}'$  did not hit  $\text{CF}$  in  $\text{F}$  (Fig. 14). This must be explained, however, as inaccurate determination of  $\text{EF}'$ , this phase line being very difficult to be determined by thermal analysis in the range 40 to 58 mole %  $\text{Ag}_2\text{SO}_4$ .

The thermal heat effect here is very small and there is practically no effect when the composition approaches 58 mole %.

The existence of the three different solid mixtures I, II, and III has been confirmed by the author<sup>12</sup> by Debye-Sherrer high temperature powder patterns.

### CONCLUSIONS

Concentration cell measurements is a sensitive method for determining phase equilibria and phase diagrams for systems with sufficient conductivity. The method is in principle a static one and has the advantages of such methods. Systems can be allowed to reach equilibrium at a certain temperature, phase changes being determined by interpolation of series of equilibrium measurements.

Concentration cell measurements can also be used as a dynamic method for the determination of a phase diagram. When continuously measuring the potentials at a constant rate of temperature change, phase changes accompanied by heat effects can be observed, because of the formation of thermocells, analogous to differential thermal analysis.

By correlating the three principles outlined phase diagrams can be constructed which are more reliable than diagrams based upon thermal analysis alone.

The requirement of a reversible electrode limits the use of concentration cells. For investigation of phase changes, however, it is not necessary to use a reversible electrode, as the changes will be observed as long as the electrode potential depends in some way on the compositions of the two half-cells.

*Acknowledgements.* The author is indebted to Professor Tormod Førland who initiated this work and has contributed generously with stimulating discussions.

### REFERENCES

1. Førland, T. and Krogh-Moe, J. *Acta Chem. Scand.* **13** (1959) 1051.
2. Førland, T. and Krogh-Moe, J. *Acta Cryst.* **11** (1958) 224.
3. Førland, T. and Krogh-Moe, J. *Acta Chem. Scand.* **11** (1957) 565.
4. Naeken, R. *Neues Jahrb. Mineral Geol. Palaeontol* **24** (1909) *Beil. Bd. 1.*
5. Strickler, H. S. and Seltz, H. *J. Am. Chem. Soc.* **58** (1936) 2084.
6. Sundheim, B. R. (Ed.) *Fused Salts*, McGraw Hill Book Co., New York 1964. Chapter by Førland, T. *Thermodynamic Properties of Fused Salts. In press.*
7. Bockris, J. O'M., White, J. L. and Mackenzie, J. D. (Ed.) *Physicochemical Measurements at High Temperatures*, Butterworths, London 1960, p. 51.
8. American Institute of Physics, *Temperature, Its Measurements and Control in Science and Industry*, Reinhold Publ. Corp., New York 1941, p. 284.
9. Hegedüs, A. J. and Fukker, K. *Z. anorg. allgem. Chem.* **284** (1956) 20.
10. Hedvall, J. A., Lindner, R. and Hartler, N. *Acta Chem. Scand.* **4** (1950) 1099.
11. Lesnykh, D. S. and Bergman, A. G. *Zh. Obshch. Khim.* **23** (1953) 373.
12. Øye, H. A. *Thermodynamic Investigation of the System  $Li_2SO_4 - Ag_2SO_4$*  (Diss.) The Technical University of Norway, Trondheim 1963.

Received October 18, 1963.